JOURNAL OF OPTOELECTRONICS AND ADVANCED MATERIALS, Vol. 11, No. 11, November 2009, p. 1681 - 1685

Wavefront aberration correction in single mode fibre systems

M. A. PAUN[a,b*], M. R. N. AVANAKI[c], G. DOBRE[a], A. HOJJAT[c], A. G. PODOLEANU[a]
[a]*Applied Optics Group (AOG), School of Physical Sciences, University of Kent, Canterbury, Kent, CT2 7NH, United Kingdom,*
[b]*Currently at Electronics Lab (ELAB), EPFL (Ecole Polytechnique Fédérale de Lausanne), CH-1015 Lausanne, Switzerland*
[c]*Research and Development Centre, School of Biosciences, University of Kent, Canterbury, Kent, CT2 7PD, United Kingdom*

A simple control loop system was built for the purpose of optimized compensation of wavefront aberrations correction using a micromachined deformable mirror controlled by PCI cards and sound card through simulated annealing algorithm implemented by using the integration of Visual C++ and MATLAB in MATLAB environment.

(Received November 3, 2009; accepted November 12, 2009)

Keywords: Optical fibre, Wavefront aberration, Single mode fibre system

1. Introduction

Adaptive optics (AO) is a technology that can be used to compensate aberrations of a light beam after propagating through the distorting medium [1]. In confocal imaging systems using single mode optical fibres (SMF) for detection, when light backscatters from a test object, it is very often aberrated and its subsequent coupling into the SMF conduit can be impaired by such aberrations, resulting in a low signal to noise ratio. Due to this, the use of adaptive optics to reduce the effect of the aberrations becomes essential especially in the applications demanding a higher signal-to-noise ratio.

First and second authors had the same contribution in this paper

An AO is made up of a wave-front sensor, like Shack-Hartmann, to measure the wave-front error, a deformable mirror (DM), to compensate the distortion, and a control loop method, to find the optimized compensation. Unfortunately such systems are expensive [1]. On the other hand, although open-loop wavefront or beam-shape control can in principle be achieved using the knowledge of a deformable mirror's influence matrix, its nonlinear characteristics make implementation of a wide range of pre-deformed shapes problematic without the use of feedback through a wavefront sensor or other forms of closed-loop control. Less expensive closed-loop methods are required for correcting distortions, such as the so-called blind optimization or sensor-less approaches [2-5]. In blind optimization algorithms, only DM is required. The algorithm operates in a closed-loop iteratively to optimize the single measurable variable towards reducing the wavefront error by changing the mirror surface.

Simulated annealing (SA) introduced in 1982 by Kirkpatrick et al. [6], is a technique for combinatorial optimization problems, such as minimizing multivariate functions [7-8] to improve the solution to the so-called Travelling Salesman Problem [9]. SA is of importance due to its efficiency with less computational complexity since all other known techniques for obtaining an optimum solution require an exponentially increasing number of steps as the problems become larger [7]. SA in comparison with iterative improvement methods [6], which are captured simply in local minima, improves the result by occasionally searching in directions that lead to worse solutions [10]. SA is however a heuristic optimization technique which does not guarantee giving the optimum value [7]. The concept of the optimization technique comes from a physical process of heating to a temperature that permits many atomic rearrangements, and then slowly cooling a substance allowing it to come to thermal equilibrium at each temperature until the material freezes an ordered crystalline structure or into a structure with the lowest energy [11]. In the context of adaptive-optical control, the simulated annealing algorithm is well-suited to the task because of its ability to independently optimize many variables at once [12].

In this paper, we aim to utilize DM and we propose an effective optimization technique to provide a simple, compact and affordable adaptive optic system to compensate aberrations introduced by distorting optical elements in optical fibre systems.

2. Materials and methods

2.1. Optical system configuration

As shown in Fig. 1, in the optical setup light is launched from a super luminescent diode (SLD) with the central wavelength of λ = 675.5 nm and $\Delta\lambda = 8.8nm$.

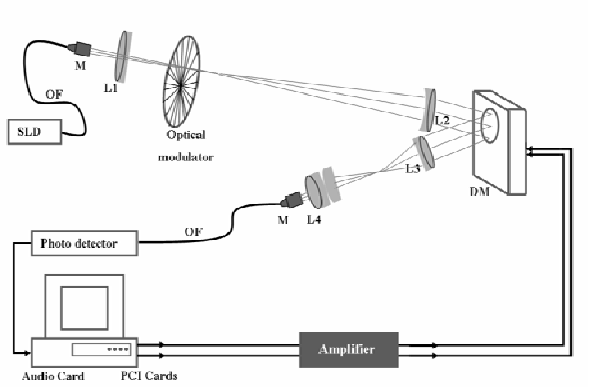

Fig. 1. Schematic of the optical system setup. (SLD: super luminescent laser diode, SMF: optical fibre, M: microscope objective, DM: 37-actuator deformable mirror, L_1-L_4: doublet lenses)

The light then is coupled into a single mode fibre (SMF). The output light from SMF is collimated by passing through a microscope objective (x10, N.A.=0.25) and guided to L_1. L_1 is a doublet lens, with focal length f_1=14 cm and diameter Φ_1=3.15 cm and L_2 is also a doublet lens with f_2=50 cm, Φ_2=2.54 cm. To match the beam diameter with that of the deformable mirror, a beam expander configuration based on L_1 and L_2 is used. With the setup we intended to achieve a beam diameter increase of approximately 3 times to cover the 15mm diameter of the mirror. The collimated beam of light is incident on the DM surface at an angle of 10º. The mirror is a micro machined membrane deformable mirror manufactured by OKO Technologies [13]. The membrane is very thin, circular in shape, and has a diameter of 15 mm. The membrane is mounted over a two-dimensional array of actuators placed in a hexagonal pattern. Any voltage difference applied between the membrane and each of 37 actuators results in the deformation of the membrane. The mirror's technology makes this mirror significantly smaller and even less expensive than piezoelectric transducer-based DMs [1] which are also used in blind optimization [14].

On the return path of the beam, two lenses are used to reduce the diameter of the beam to allow its coupling into a SMF; L_3 and L_4. They are doublet lenses with f_3= 10 cm, Φ_3= cm and f_4= 5 cm, Φ_4= cm, respectively. The light then is injected into the SMF through the x10 microscope objective. The output light is focused on the end of the fibre optic and from the other end is collected by an avalanche photodiode (Hamamatsu avalanche photodiode C5460-01, spectral response range between 400-1000nm and the typical cut-off frequency at 100 KHz). The electrical signal obtained from the photodetector is coupled into the computer sound card input port (SIP) (microphone port) and to an oscilloscope for signal monitoring.

SIP allows the photodetector signal to be recorded onto the personal computer (PC) in real time. Owing to this, we employed a mechanical chopper somewhere in the beam path to modulate the signal and therefore to make it easily detectable by the high pass filtering sound card. We operated the mechanical chopper at 100 Hz which is much less than the maximum change rate of the actuators´ voltage (>1kHz) [13].

2.2. Signal processing flow

From a signal processing point of view, the system includes the SLD, optical system excluding the mirror, detector, SIP, MATLAB as the processing unit centre, PCI cards and the DM. Signal from the SIP is gathered using MATLAB for data acquisition in real time. The signal is rectified and processed in the optimization algorithm. The output of the algorithm is a set of 37 values which are sent to the DM. The values are in the range between 0 and 255. We employ two 24-channel 8-bit PCI DAC cards and write 8-bit values to the base address of each card which results in the corresponding analogue value on the channels of the PCI card's output. As we intended to manage the input and output signals in a single programming environment, we converted the port controller code written in VC++ to MATLAB using mex file [14].

The analogue voltages generated on the output of the PCI cards are amplified linearly to the range of 0 to 193V. The voltages are then applied simultaneously to the 37 actuators of the mirror, which results in a certain shape of the membrane surface.

2. 3. The optimization schedule

In this study, the cost function is defined as the difference between the new intensity and the highest intensity detected up to that point, which we call Current Maximum Intensity (CMI). The variables are the 37 components of a vector sent to the actuators. The vector controls the actuator voltages. The flowchart of our SA-based algorithm designed to find the best mirror shape is given in Fig. 2.

We use an artificial parameter which we call the "synthetic temperature" to determine how often the system switches between local and global search. The initial value of the synthetic temperature has to be high enough to let the algorithm jump up to anywhere in the variable space. We experimentally considered the initial temperature (melt temperature) to be 1000 and the final (frozen) temperature to be 0.001. The algorithm is started with sending a random set of 37 values as actuators' voltages between zero and 255. A uniformly distributed pseudo-random function is chosen to generate the random values [14].

The maximum intensity is set to zero at the beginning. From now on, the algorithm operates in its *ordinary optimization loop* (OOL) while the temperature is examined to see whether or not it is still less than the frozen temperature. The shape of the mirror changes according to the actuator voltages and this results in a new value of the light intensity detected. If the intensity is greater than the CMI value, it becomes the new CMI and also the voltage vector is saved as the best vector.

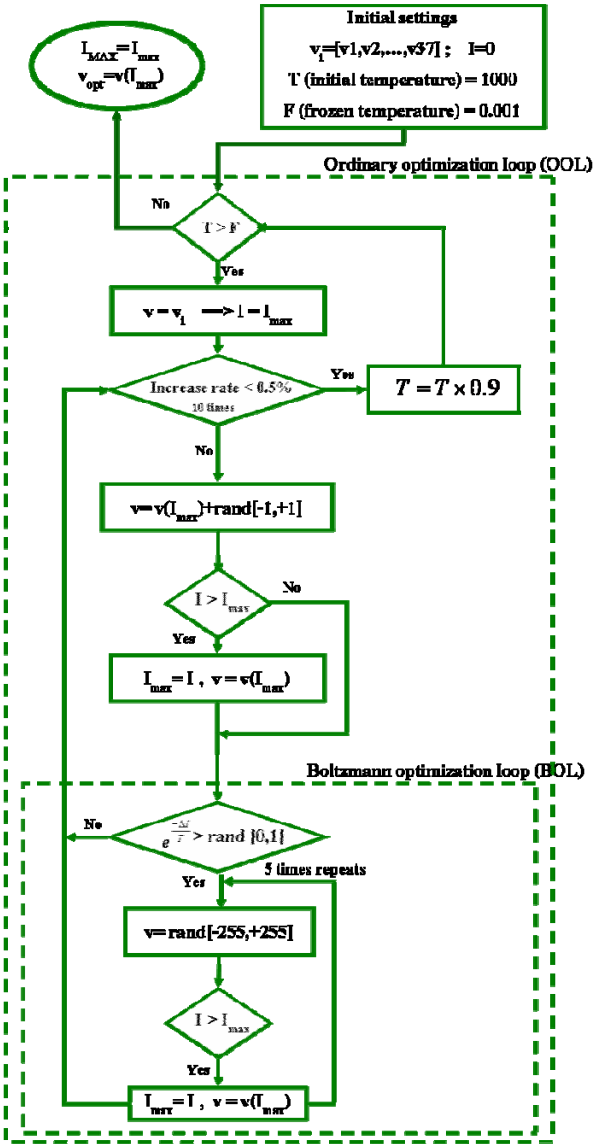

Fig. 2. Flowchart diagram of our simulated annealing algorithm applied to wavefront aberration optimization

At each temperature, the OOL is continued until we reach the situation where in 10 successive iterations the rate of increase of the intensity becomes less than a threshold value. We defined an allowed variation at each temperature which is constant for a determined number of temperatures. As shown in Figure 3-a, the threshold values are decreased by 10% for each temperature step decrease. Accordingly the allowed variation is progressively smaller. As a result, the thermal equilibrium condition of the algorithm is obtained in a smaller range of intensity variation.

The cooling schedule as shown in Figure 3-b is based on $T_{new}=0.9T_{old}$; in this study, the number of cooling-down steps based on our choice of initial and final temperatures is 132 steps. In each iteration of the OOL, the values of actuators voltages are updated around the best voltage by adding/reducing one unit to/from the voltages individually and in a random manner.

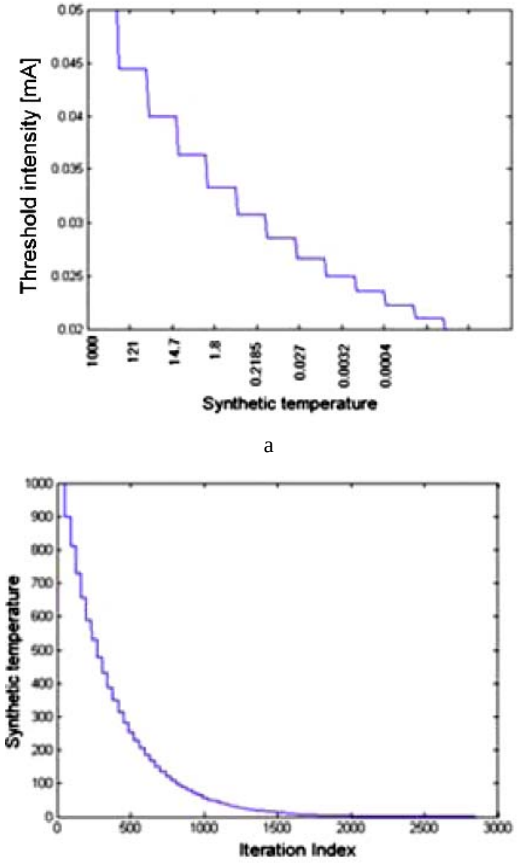

Fig. 3. (a) Threshold intensity decrease profile with temperature. (b) Temperature reduction profile during the simulated annealing process based on successive temperature reductions given by $T_{new}=0.9T_{old}$.

In the OOL the Boltzmann probability function is compared with a random value in the interval 0 and 1. If the probability is greater than the random value we let the algorithm jump to random points in the variable space 5 times (this value was obtained experimentally), by changing the voltage vector in the range of 0 to 255. If the intensity at this stage is higher than the CMI, it becomes the new CMI and the corresponding voltage set is recorded and becomes the best voltage set. After reaching the thermal equilibrium in each temperature, the system temperature is decreased.

The process terminates when the temperature becomes lower than the frozen temperature. In the end, the optimal shape of the mirror is determined by the best voltage obtained from the algorithm which leads to producing the highest obtainable intensity with the optical setup.

3. Results and discussion

The algorithm was tested on a 2GHz Pentium IV computer with 1GB RAM. The progression of intensity along the simulated annealing algorithm in finding the more appropriate shape of the mirror with higher intensity is given in Fig. 4.

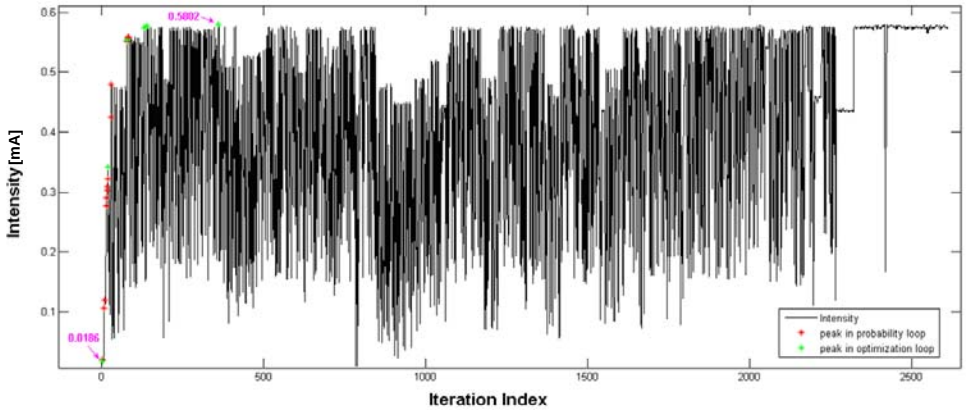

Fig. 4. Output intensity amplitude profile recorded from audio card during 2600 iterations in our simulated annealing algorithm. The minimum and maximum intensities are pointed out on the graph by arrows. The red starts show the improved intensity obtained from the ordinary optimization loop and the green starts show the improved intensity obtained from the Boltzmann loop.

As shown in Fig. 4, the output intensity of the system is increased from 0.0186 mA to 0.5802 mA which shows a 31-fold increase. We can not claim that the algorithm is able to enhance the DOCI by the order of around 31 times, but we can say if the optical system is involved with a static aberration, the proposed algorithm is able to find an appropriate shape of the mirror to correct and compensate the aberration such that the system achieves the highest possible intensity. The progression of the intensity in Fig. 4 in the first stages of the algorithm is very fast such that in the first 82 iterations, the intensity in 16 steps has been improved 30 times whereas in the next 57 iterations we had only two steps which resulted only 1.12 times improvement. The rest of the iterations do not improve the intensity any further.

As seen in Fig. 4, considering the application of the Boltzmann probability condition resulted in large variations of the intensity. In this loop the algorithm looks for a better intensity value throughout the variable space by changing the voltage set values (randomly in the interval between 0 and 255). The number of improved intensities indicated by red starts on Fig. 4 shows the significance of the use of Boltzmann probability scheme. As the algorithm reaches to the lower temperature the probability condition is fulfilled fewer times and the OOL operates without going through the Boltzmann loop. We examined our algorithm for a similar setup to the one shown in Figure 1 on 14 different runs and we obtained the results in Table 1.

Table 1. Results of successively running the developed simulated annealing algorithm for 14 times. The whole number of samples in all experiments is 2845. Runtime (95%I_{max} (s)) in the table, shows the time required to reach 0.95 of the maximum intensity. I(v_{best}), shows the intensity when we sent the final best voltage set to the mirror after finishing the algorithm.

Ex. #	I_{max} (mA)	I_{max}/ I_{min}	Number of peaks found in Boltzmann loop	Number of peaks found in ordinary optimization loop	runtime (min)	runtime (95%I_{max} (s))	I (v_{best})
1	0.5760	3.45	20	29	28	66.7/	0.5735
2	0.5757	3.6	17	38	27	314	0.5688
3	0.5756	4.39	14	24	27	161	0.5671
4	0.5750	3.45	13	14	26	20	0.5672
5	0.5748	2.5	13	20	26	21.2	0.5692
6	0.5747	3.79	15	21	26	20	0.5721
7	0.5724	5.17	14	36	27	223	0.5686
8	0.5716	4	24	39	27	133	0.5703
9	0.5714	5.2	18	31	25	203	0.5601
10	0.5602	4.2	14	29	27	544	0.5505
11	0.5575	4.6	13	411	25	499	0.5480
12	0.5454	4.13	17	45	24	277	0.5298
13	0.5353	6	13	42	25	168	0.5283
14	0.5280	4.28	8	19	25	72	0.5109

In some SA applications, due to time limitations, it is not possible to obtain the optimum answer in the allocated time [6]. Further ongoing research is aimed at investigating the optimum run time on our type of optical system, which will allow faster optimization.

4. Conclusions

In summary, we have demonstrated an efficient method for optimization of fiber optic systems using a micromachined membrane deformable mirror in conjunction with our simulated annealing algorithm. We configured an adaptive optics setup (Figure 1) and examined the optimization algorithm successfully. We used simple and inexpensive computer interface (audio card for receiving and PCI DAC cards for sending signals) in single programming environment, Matlab. We showed that the algorithm is quite promising in finding the global maximum intensity and that is reproducible by running it 14 times and recording the results (Table 1). We showed that with this configuration, a compact, inexpensive and simple optimization approach is achievable. We also mentioned the limitation of the algorithm in terms of timing and that of is an application-oriented.

We conclude that while this technique is unlikely to find the optimum solution, it can often find a very good solution. We have plans to expand the use of this approach in confocal microscopy and optical coherence tomography in order to remove both aberrations caused by the interface optics and those caused by target itself, which will enable deeper exploration of certain types of specimens.

References

[1] M. L. Plett, P. R. Barbier, D. W. Rush, Appl. Opt., **40,** 327 (2001).
[2] M. Booth., Optics Express, **14,** 1339 (2006).
[3] E. Grisan, F. Frassetto, V. Da Deppo, et al., Appl. Opt. **46,** 6434 (2007).
[4] S. Zommer, E. Ribak, in: Proc. 3rd International Conference on Visual Optics, Mopane 2006, (Mopani Camp, South Africa), 2006
[5] C. D. Toledo-Suárez, M. Valenzuela-Rendón, H. Terashima-Marín, et al. in: Proc 9th annual conference on Genetic and evolutionary computation, London, England, 2007, p. 1436-1443
[6] O. Soloviev, M. Loktev, G. Vdovin, Adaptive Optics Product Guide, April 2009 edn. (OKO technology, 2009), http://www.okotech.com
[7] P. Yang, Y. Liu, W. Yang, et al., Opt. Commun. **278,** 377 (2007).
[8] MathWorks, M.: The Language of Technical Computing, http://www.mathworks.com
[9] Lawler, E. L., Rinnooy-Kan, A., Lenstra, J. K. et al.: The traveling salesman problem: A guided tour of combinatorial optimization, John Wiley & Sons Inc, 1985
[10] R. Rutenbar, IEEE Circuits Devices Mag. **5,** 19 (1989).
[11] Fang, M., Master Project, University of Bridgeport, USA, 2000
[12] R. El-Agmy, H. Bulte, A. Greenaway, et al., Optics Express, **13,** 6085 (2005).
[13] S. Kirkpatric, C. Gelatt, M. Vecchi, Science **220,** 671 (1983).
[14] R. Carr, "Simulated Annealing", From MathWorld – A Wolfram Web Resource, created by E. W. Weisstein, http://mathworld.wolfram.com/ SimulatedAnnealing.html

*Corresponding author: maria-alexandra.paun@epfl.ch